Available online at www.sciencedirect.com
ScienceDirect
International Journal of Mass Spectrometry 266 (2007) 8–14
International Journal of Mass Spectrometry
www.elsevier.com/locate/ijms

Transition state ring sizes in H-transfers in closed shell aliphatic cations

Charles E. Hudson [a], Lawrence L. Griffin [b], David J. McAdoo [a,*]

[a] *Department of Neuroscience and Cell Biology, University of Texas Medical Branch, 301 University Blvd., Galveston, TX 77555-1043, United States*
[b] *Department of Marine Sciences, Texas A&M University at Galveston, Galveston, TX 77553, United States*

Received 11 April 2007; received in revised form 5 June 2007; accepted 5 June 2007
Available online 15 June 2007

Abstract

We use theory to determine the relative rates of 4-, 5- and 6-membered ring H-transfers in closed shell cations, a comparison not possible experimentally due to interference from competing processes. H-transfers of increasing ring size were characterized by ab initio, density functional and/or RRKM studies of $CH_3N^+H{=}CH_2$, $NH_2CH{=}N^+HCH_3$, $NH_2CH_2N^+H{=}CH_2$, $NH_2CH_2CH_2N^+H{=}CH_2$, $N^+H_2{=}CHCH_2NHCH_3$ and $CH_3NHCH_2NH^+{=}CH_2$. The critical energies for these reactions decreased and the rates thereof increased dramatically with increasing H-transfer ring size. Transition state ring strain and avoiding orbital symmetry constraints together produce the same sequence of reaction rates (6 > 5 > 4 membered ring preference) and critical energies (4 > 5 > 6 membered ring order) in open and closed shell organic cations. Twisting around double bonds during H-transfers breaks conjugation and allows the reactions to bypass orbital symmetry constraints.

Keywords: H-transfer isomerizations; Closed shell cations; Intrinsic reaction cocodinate; Ring sizes; RRKM

1. Introduction

H-transfers are important in many areas of chemistry. Competition between H-transfers through transition states of different ring sizes has long been of interest in gas phase ion chemistry [1,2]. Odd electron/open shell ions undergo specific, predictable H-transfers and dissociations, e.g., the McLafferty rearrangement, and are of substantial utility for compound identification and structure determination [3,4]. Competition among H-transfers by different ring-sized transition states in open shell species has been characterized experimentally [1] and theoretically [2], establishing a preferred order 6 > 5 > 4-membered ring transition states. Closed shell ions also undergo extensive H-shifts, but due to extensive competition from ion-neutral complex-mediated H-transfers and other reactions [5,6], specific H-transfers are difficult to characterize experimentally in those ions. We recently characterized a closed shell analog of the typical McLafferty rearrangement and smaller ring H-transfers in $CH_2{=}N^+HCH_2CH_2CH_3$ by computational methods (Scheme 1) [7]. We found that this "McLafferty rearrangement" differs from McLafferty rearrangements in open shell species in that the dissociation of $CH_2{=}N^+HCH_2CH_2CH_3$ is concerted (Scheme 1) [7], whereas in open shell species the McLafferty rearrangement usually involves formation of an intermediate followed by dissociation [8,9].

We also found that the 5-membered ring H-transfer in Scheme 1 is slightly higher in energy than the 4-membered ring H-transfer, substantially in the opposite direction from the relative energies of those two types of reactions in open shell ions [2,10,11]. A high energy apparent intermediate is accessed by 5-membered ring H-transfer (Scheme 1) [7], making uncertain the degree to which the associated transition state energy is due to the high energy of the immediate products of the reactions versus ring strain. To resolve this, we here use ab initio, density functional and RRKM theories to define better the intrinsic preferences for H-transfers in the closed shell reactions depicted in Scheme 2.

2. Calculations

Energies and geometries of stationary points were obtained using the Gaussian 03 program package [12]. Geometries were obtained by B3LYP/6-31G(d), B3LYP/6-311G(d,p) and QCISD/6-31G(d) theories and basis sets. Energies were

* Corresponding author. Tel.: +1 409 772 2939; fax: +1 409 772 3222.
E-mail address: djmcadoo@utmb.edu (D.J. McAdoo).

1387-3806/$ – see front matter © 2007 Elsevier B.V. All rights reserved.
doi:10.1016/j.ijms.2007.06.008

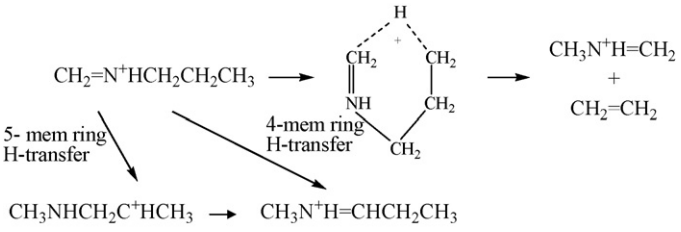

Scheme 1.

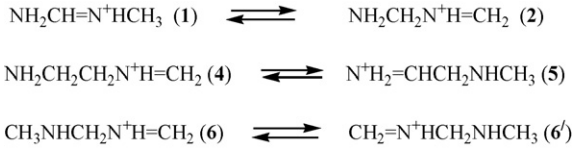

Scheme 2.

obtained with the same levels of theory and basis sets as the corresponding geometries, except QCISD(T)/6-311G(d,p) energies were obtained at QCISD/6-31G(d) geometries. Species were considered to be stable when they had only positive vibrational frequencies, and to be transition states when they possessed one imaginary vibrational frequency. Zero point energies were obtained by multiplying zero point energies derived from B3LYP/6-31G(d) frequencies by Scott and Radom's scaling factor of 0.9806 [13]. Reaction pathways were traced by intrinsic reaction coordinate (IRC) methods [14,15] utilizing B3LYP theory and the 6–31G(d) basis set.

Rate constants were obtained as a function of energy by RRKM theory [16]. For those calculations, the vibrational frequencies computed at the B3LYP/6-31G(d) level were scaled by factors of 1.0013 for frequencies below 600 cm^{-1} and by 0.9614 for frequencies above 600 cm^{-1} [13].

3. Results and discussion

3.1. Energies of critical points

Our discussion emphasizes our QCISD(T)/6-311G(d,p) results, as those are from the highest level and probably the most accurate calculations that we applied (Table 1). Except for TS(**4** → **5**), the energies produced by the two highest levels of theory that we utilized, QCISD(T)/6-311G(d,p) and B3LYP/6-311G(d,p) energies agree within 20 kJ mol^{-1}, attesting to the reasonableness of our results.

The QCISD(T)/6-311G(d,p) critical energy for 4-membered ring **cis-1** → **2** is 336.9 kJ mol^{-1} and that for **trans-1** → **2** is 354.5 kJ mol^{-1}, the highest energies we found among the H-transfers considered. The critical energy for the reverse reaction, **2** → **cis-1**, is 235.9 kJ mol^{-1} at the same level of theory. **Trans-1** is 3.6 kJ mol^{-1} higher in energy than is **cis-1** (Table 1). The critical energy for the 1,3-H-shift $CH_3N^+H{=}CH_2 \rightarrow CH_2{=}N^+HCH_3$ found previously at the same level of theory is 262.5 kJ mol^{-1} [7], between the energies for **1** → **2** and **2** → **1**. $CH_3N^+H{=}CH_2 \rightarrow CH_2{=}N^+HCH_3$ is probably the most representative 4-membered ring critical energy that we have obtained, given the identity of the reactants and products and large difference between the critical energies for **1** → **2** and **2** → **1**. The critical energies for all of these 4-membered ring reactions are substantially higher than the critical energies for

Table 1
Energies of transition states for different ring size H-transfers

	ZPE	B3LYP/6-31G(d)	B3LYP/6-311G(d,p)	QCISD/6-31G(d)	QCISD(T)/6-311G(d,p)
cis-$NH_2CH{=}N^+HCH_3$ (**cis-1**)	260.6	−189.699797	−189.758598	−189.112373	−189.256296
$NH_2CH_2N^+H{=}CH_2$ (**2**)	258.0	−189.654643	−189.713559	−189.071966	−189.216835
E_{rel}[a]		116.0	115.6	103.5	101.0
TS(**cis-1** → **2**)	245.1	−189.565315	−189.625722	−189.968998	−189.122070
TS(**cis-1** → **2**)[a]		337.6	333.4	360.9	336.9
TS(**2** → **cis-1**)[a]		221.6	217.6	257.4	235.9
Trans-1[a]	260.1	2.1	2.4	3.6	3.6
TS(**trans-1** → **2**)[a]		372.0	368.0	379.0	354.5
$TS(CH_3N^+{=}CH_2 \rightarrow CH_2{=}N^+HCH_3$[b]		271.7	265.6	284.2	262.5
$NH_2CH{=}NHCH_2^{\bullet+}$ (**3**)	223.4	−189.036049	−189.094835	−188.457258	−188.592358
$H^{\bullet}$		−0.500272	−0.502156	−0.498233	−0.499809
$NH_2CH{=}NHCH_2^{\bullet+} + H^{\bullet}$	223.4	−189.536321	−189.596991	−188.955491	−188.092167
E_{rel}[a]		392.0	387.1	374.7	393.7
$NH_2CH_2CH_2NH^+{=}CH_2$ (**4**)	334.4	−228.978573	−229.047077	−228.259911	−228.439726
$N^+H_2{=}CHCH_2NHCH_3$ (**5**)	332.0	−228.970582	−229.039283	−228.245872	−228.425347
E_{rel}[c]		18.7	18.0	34.5	35.4
TS(**4** → **5**)	322.6	−228.921229	−228.990052	−228.184000	−228.372759
TS(**4** → **5**)[c]		138.8	137.9	187.5	164.0
TS(**5** → **4**)[c]		120.1	119.9	153.0	128.6
$CH_3NHCH_2NH^+{=}CH_2$ (**6**, **6′**)	329.4	−228.963949	−229.030284	−228.240935	−228.419272
TS(**6** → **6′**)	326.3	−228.943354	−229.008897	−228.208897	−228.395789
TS(**6** → **6′**)[d]		51.0	55.1	81.0	58.6

[a] Relative to **cis-1** = 0 kJ mol^{-1}.
[b] Ref. [7].
[c] Relative to **4**.
[d] Relative to **6**.

5- and 6-membered ring H-shifts (see following), as is generally the case for 4-membered ring H-transfers in open shell ions [1,2,8,10].

The critical energy of **4** → **5** is 164 kJ mol^{-1}, 173 kJ mol^{-1} less than the critical energy of **1** → **2**. The critical energy for **5** → **4**, 129 kJ mol^{-1}, is also well below the critical energies for **1** → **2** (337 kJ mol^{-1}) and **2** → **1** (236 kJ mol^{-1}). Thus, the energies required for 5-membered ring H-transfers by these ions are much lower than those for 4-membered ring reactions. However, the opposite order can occur in closed shell ions, e.g., passage through the high energy $CH_3NHCH_2C^+HCH_3$ requires more energy than 4-membered ring isomerization to the highly stabilized $CH_2{=}N^+HCH_2CH_2CH_3$ (see Section 1) [7]. Effects of differences between energies of reactants and products were minimized by choosing **4** → **5** and **5** → **4**, reactions having reactants and products of similar stabilities (differing by 35.4 kJ mol^{-1}, Table 1), and much lower energies than connecting transition states.

The QCISD(T)/6-311G(d,p) activation energy for the degenerate 6-membered ring H-transfer **6** → **6′** is 58.6 kJ mol^{-1}, substantially lower than those for the 5-membered ring processes **4** → **5** and **5** → **4**, and even further below the critical energies for the four-membered ring reactions **1** → **2**, **2** → **1** and the degenerate isomerization of $CH_3N^+H{=}CH_2$. Present results give the ring size reaction preference order 6 > 5 > 4 for systems studied, matching that for open shell species [1,2]. These were confirmed by following RRKM calculations. This order is likely general for closed shell systems as long as no unusual influences are present. Given that each transition state in the present work is substantially higher in energy than the associated reactants and immediate products and that no intermediates were found in the reactions studied, energies of intermediates do not influence the critical energies for reactions characterized here.

Critical energies for H-transfers in several series of ions are given in Table 2. In three of the four series, the preference order of reaction rates is 6 > 5 > 4 membered rings.

3.2. Relative RRKM reaction rates

To establish the relative rates of H-transfer by different ring sizes, we utilized RRKM theory to calculate rate constants as a function of internal energy (Fig. 1). According to the results, at internal energies of 350 kJ mol^{-1} 4-membered ring **1** → **2** is 7–8 orders of magnitude slower than 5-membered ring reactions **4** → **5** and **5** → **4**, and ca. 9 orders of magnitude slower than **6** → **6′**. The 6-membered ring **6** → **6′** is about 7 orders of magnitude faster than the 5-membered ring H-transfer **4** → **5** near the threshold for the latter. However, the rate constants for **5** → **4** and of **6** → **6′** approach each other to within an order of magnitude at high energies (Fig. 1). Thus, as in open shell ions, 6-membered ring H-transfers are faster than 5- and 4-membered ring H-transfers in the closed shell ions studied here, and 5-membered ring H-transfers are much faster than 4-membered ring H-transfers, particularly at low energies.

Reaction **1** → **2** is orders of magnitude slower than its reverse up to internal energies above 500 kJ mol^{-1}. Similarly, near threshold 5-membered ring **4** → **5** is about 2–3 orders of magnitude slower than its reverse. However, the rate constants for the last two reactions converge as the excess energy in the system approaches 500 kJ mol^{-1}. As expected, these data reflect that the relative critical energies of the reactions are important determinants of their rates, the higher its critical energy, the slower the reaction.

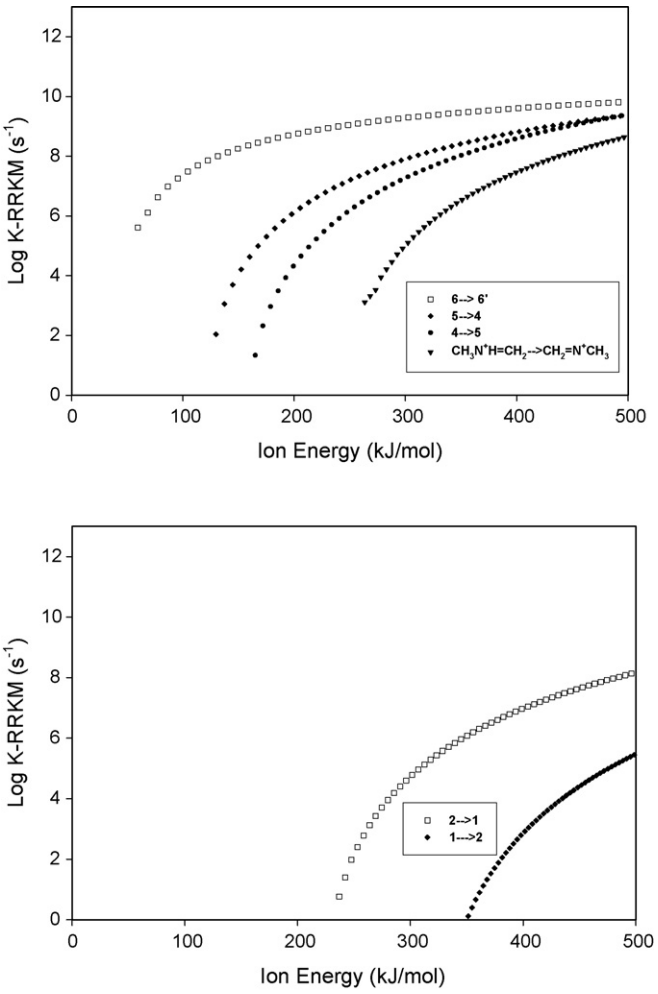

Fig. 1. Upper panel: RRKM rate constants obtained using B3LYP/6-31G(d) frequencies and QCISD(T)/6-311G(d,p) critical energies. Reactions for which plots are shown are $CH_3N^+H{=}CH_2$ → $CH_2{=}N^+HCH_3$, $NH_2CH_2CH_2N^+H{=}CH_2$ (**4**) → $N^+H_2{=}CHCH_2NHCH_3$ (**5**), $N^+H_2{=}CHCH_2NHCH_3$ (**5**) → $NH_2CH_2CH_2N^+H{=}CH_2$ (**4**) and $CH_3NHCH_2N^+H{=}CH_2$ (**6**) → $CH_2{=}N^+HCH_2NHCH_3$ (**6′**). These represent 4-, 5- and 6-membered ring H-transfers, respectively. Lower panel: Dependence of RRKM rate constants on ion internal energy for $NH_2CH{=}N^+HCH_3$ (**1**) → $NH_2CH_2N^+H{=}CH_2$ (**2**) and its reverse.

Table 2
H-transfer critical energies (kJ mol^{-1}) for various ring size transition states

H-transfer ring size	4	5	6
(Present: Table 1)	337	164	58.6
($CH_2{=}N^+HCH_2CH_2CH_3$)[a]	241, 262	256	173
$^{\bullet}(CH_2)_nNH_3^{+}$[b]	132	57	9
$C_nH_{2n}O^{+}$[c]	196	91	32

[a] Ref. [7].
[b] Ref. [2]. $CH_3(CH_2)_{n-1}NH_2^{\bullet+}$ → $^{\bullet}(CH_2)_nNH_3^{+}$.
[c] Refs. [10] and [11]. $CH_3C(=OH^+)(CH_2)_n^{\bullet}$ → $CH_3C(=O^{\bullet+})(CH_2)_{n-1}CH_3$.

3.3. Geometries of stationary points

Geometries of reactants and transition states were obtained by B3LYP and QCISD theories. The following diagram gives the designations of the atoms we will use in discussing TS(**1** → **2**) and its IRC.

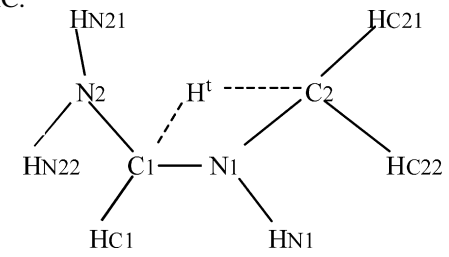

The geometries of **1**, **2** and TS(**1** → **2**) obtained by QCISD/6-31G(d) theory are depicted in Fig. 2. H^t is closer to C1 (1.224 Å) than to C2 (1.641 Å) at the transition state for the 4-membered ring H-transfers that interconvert **1** and **2**. The N1C1H^tC2 dihedral angle in the H-transfer ring in TS(**1** → **2**) is 6.2° {QCISD/6-31G(d) theory; 4.40° by B3LYP/6-31G theory}, so the transition state ring approaches planarity. The dihedral angles between the hydrogens on C2 and the C2N1C1 plane are 114.4° and −81.4° at TS(**1** → **2**). H^t passes similar but unequal distances from HC21 and HC22 as it approaches/leaves C2 (Fig. 2). (The distances from H^t to the methylene hydrogens are 2.23 and 1.95 Å). The approach to/departure from C1 is similar to that for C2, as the N2C1N1C2 dihedral angle = 115.5° and the HC1C1N1C2 dihedral angle = −108.7°. These values place N2 and HC1 on opposite sides of the H^tC2N1C1 "plane" at the transition state. HN1 also projects out of the ring "plane", as at the transition state, the sum of the bond angles about N1 is 315.8°, significantly less than the 360° the sum would be if the atoms bonded to N1 were planar.

Given interest in 4-membered ring H-transfers across double bonds [10,17–20], we characterized the interconversion of **1** and **2** further by IRC calculations. Pertinent dimensions are traced through the course of the reactions in Fig. 3. All atoms are planar at the starting point of the reaction, cis-$NH_2CH{=}N^+HCH_3$ (**1**), except HC21 and HC22 are above and below the molecular "plane". At the transition state on the IRC, the HC21C2N1C1 and HC22C2N1C1 dihedral angles are 120° and −75°, respectively, similar to the above QCISD results for this transition state. At the endpoint **2**, the same dihedral angles are −179.2° and 0.75°, demonstrating near-planarity of the atoms attached to the double bond. HC21 and HC22 move in the same direction during reaction, i.e., the CH_2 rotates (Fig. 3, middle). As in the QCISD/6-31G(d) transition state, $N2H_2$ is out of the plane of the double bond.

In the initial portion of the IRC for **1** → **2**, H^t leaves C2 as it approaches C1 (Fig. 3). Between TS(**1** → **2**) and **2**, H_t completes a normal bond to C1 as it continues to move away from C2. From **1** to the transition state, the N1C1H^tC2 dihedral angle decreases from 34.95° at **1** to 4.40°, a local minimum in this parameter, by rotation of the methyl (Fig. 3, bottom). Beyond the transition state, the dihedral angle N1C1H^tC2 first increases to 8.56° from the transition state and then declines to −5.28° at **2**. Thus, after the transition state is passed, H^t stays fairly

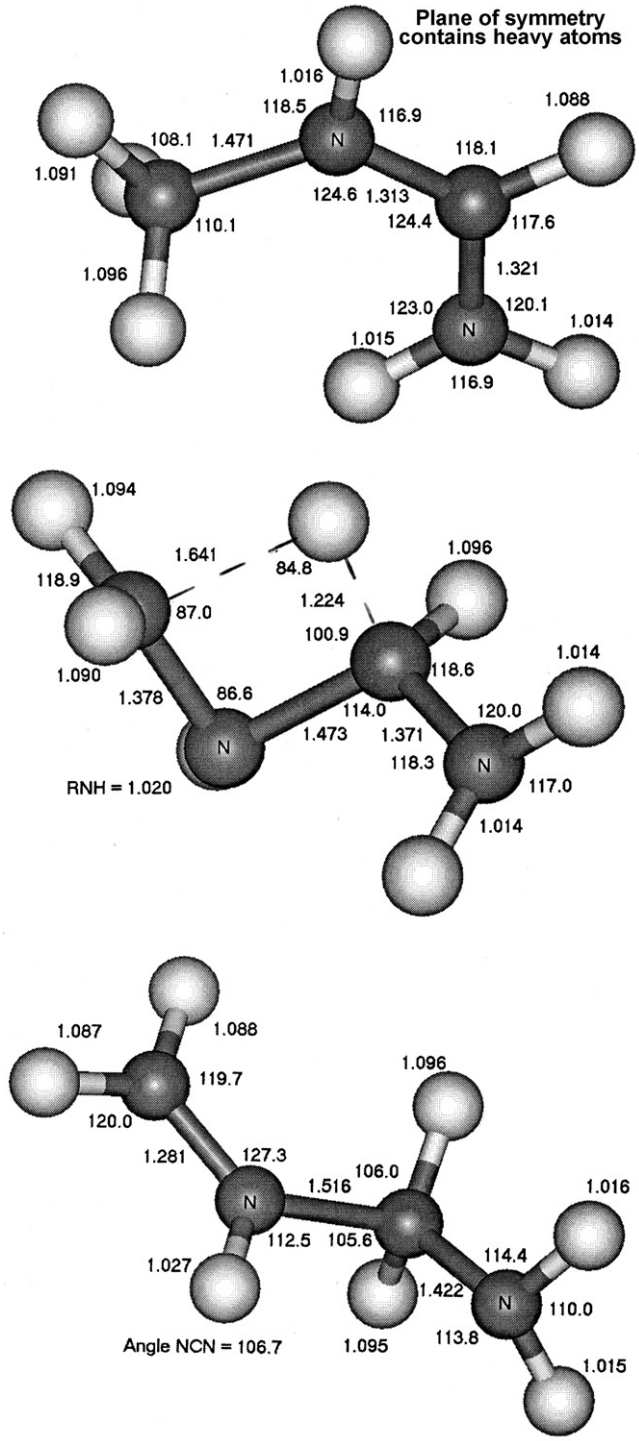

Fig. 2. Structures for $NH_2CH{=}N^+HCH_3$ (**1**), $NH_2CH_2N^+H{=}CH_2$ (**2**) and the transition state connecting them, as obtained by QCISD/6-31G(d) theory.

close to the N1C1C2 plane. Similarly, the H^tC2N1C1 dihedral angle (not shown) goes from −27.05° at **1** to −5.17° at the transition state and crosses the plane and reaches 12.4° at **2**. Thus, beyond the transition state, H^t moves near the C2N1C1 plane to C1. Also in the course of **1** → **2**, the HC21C2N1C1 dihedral angle starts at 181.3°, declines steadily to 119° near the transition state and ends at 182.6° at **2**. Thus, H21 starts very

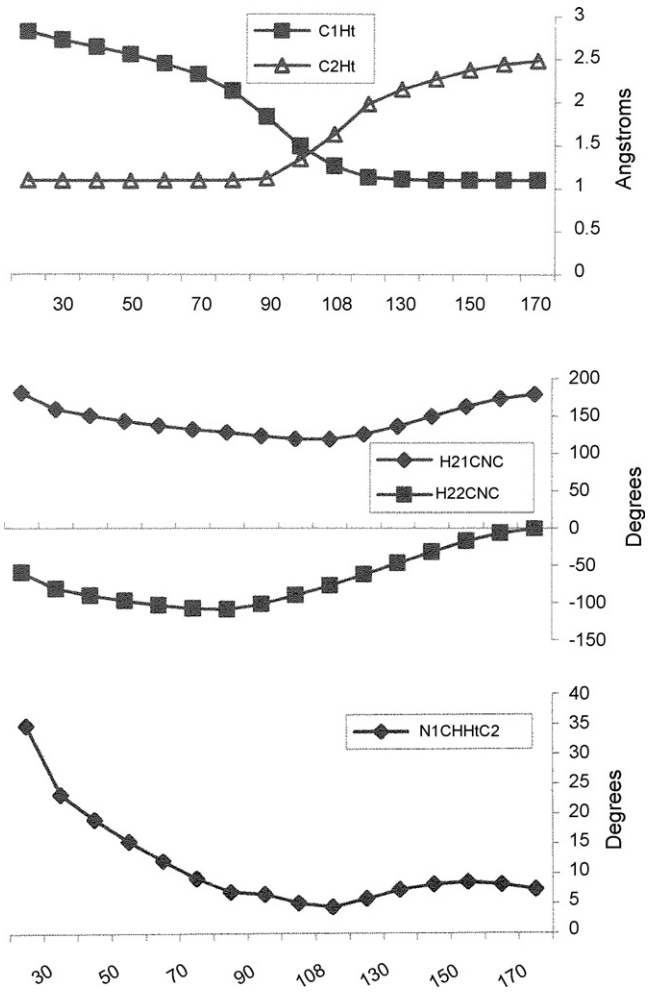

Fig. 3. Selected angles and a bond distance obtained by an IRC trace using B3LYP/6-31G(d) theory over the course of $NH_2CH{=}N^+HCH_3$ (**1**) → $NH_2CH_2N^+H{=}CH_2$ (**2**) (left to right). The top traces are the distances between the transferring hydrogen and the carbons it leaves and approaches in the course of the reaction. The middle traces are the degrees of the HC21C2N1C1 and HC22C2N1C1 dihedral angles. The bottom trace is the change in the N1C1H^{t}C2 dihedral angle made up of the atoms of the 4-membered ring transition state for **1** → **2**. The decline in the N1C1H^{t}C2 angle at the beginning of that trace reflects rotation of the methyl group. Note that the changes in the dimensions in all three panels occur in a parallel fashion.

close to the plane of **1**, moves away from that plane as H is transferred and moves back to planarity with the double bond at the end of the reaction. H22CNC starts from its geometry in methyl (−59.9° at **1**), decreases to −108.9° and then rises to −80.1° at the transition state. Past the transition state, it rises until it passes through 0–2.58°, i.e., ending essentially in the plane of the double bond in **2**. During H^t transfer, the dihedral angles for the atoms on the origin and destination carbons adjust to accommodate changes between sp^2 and sp^3 hybridization.

That H^t does not approach CH_2 in a plane bisecting the latter contrasts to H^t attacking/leaving methylene in a bisecting skeletal plane in 1,3-H-shfts in $CH_3O^+{=}CH_2$ [17,19], $CH_2{=}CHOH^+$,$^\bullet CH_2{=}C(OH)_2^{\bullet+}$ and $CH_3C(OH^{\bullet+}){=}CH_2$) [10,19]. CH_2 rotation to ca. 90° and H-transfer occur largely in separate stages in the latter reactions. However, similar to the interconversion of CH_3CHO and $CH_2{=}CHOH$ [19] and the degenerate H-shift between the carbons of $CH_3C(OH^{\bullet+}){=}CH_2$ [10], rotation and H-transfer in TS(**1** → **2**) are simultaneous, parallel processes. Both of the former reactions are suprafacial, in contrast to simple predictions of Woodward-Hoffmann theory [20]. In the interconversion of **1** and **2**, although H$_t$ crosses the plane, it only does so far from TS(**1** → **2**) after methyl formation is essentially complete. We hypothesize that **1** → **2** avoids violating orbital symmetry because at the transition state the bonds around C1, N1 and C2 are substantially non-planar, i.e., not conjugated, a situation in which suprafacial H-transfer would not violate conservation of orbital symmetry. We attribute the high energies required to accomplish this to the substantial distortions required to reach this transition state geometry. We believe that rotations about π-bonds in 1,3-H-shifts across double bonds break off conjugation in order to bypass Woodward-Hoffman constraints, whether they occur synchronously or in stages.

According to Table 1, 18–34 kJ mol^{-1} less energy is required to convert **1** to **2** than to dissociate **1** to $NH_2CH^+{-}NH{=}CH_2$ (**3**) + H$^\bullet$. This raises the possibility that TS(**1** → **2**) approximates a [$NH_2CH{=}NH{-}CH_2^{\bullet+}\cdots H^\bullet$] pair, i.e., that the transition state energy is largely determined by the energy required to break the CH bond [21]. However, **3** is completely planar, whereas, as already noted, in TS(**1** → **2**) the atoms attached to C1, C2 and N1 are well outside the plane of those atoms. Thus, **1** → **2** does not resemble a dissociation-re-association.

The atoms bonded to the π-atoms are planar in **4** and nearly planar in **5**. In **4** the HCNC dihedral angles starting with the external methylene hydrogens are 0.4° and −179.6°, demonstrating planarity about the double bond. The remaining atoms in that ion are outside of this plane. The dihedral angles going from the methylene hydrogens to the second C in the $H_2N{=}CH{-}C$ moiety in **5** equal −170.8° and 7.45°, respectively); these combine to 178.2°, so the methylene is essentially planar. TS(**4** → **5**), **4**, **5** and TS(**5** → **4**) are represented in Fig. 4. The ring in the transition state for **4** → **5** is very non-planar, with a dihedral angle of 34.7° for ring atoms CNCH and a dihedral angle of −34.4° for ring atoms NCHC. At TS(**4** → **5**), H$_t$ is slightly closer to the internal carbon (1.345 Å) than to the terminal carbon (1.452 Å).

At TS(**6** → **6′**), H$_t$ is equidistant from the carbons it is approaching and leaving, and the overall structure has a plane of symmetry that contains H$_t$, the middle carbon and the two hydrogens on the latter (Fig. 5). The dihedral angles CNCH$_t$ in both directions from the middle carbon in TS(**6** → **6′**) are −46.1°. Ion **6** is planar about its double bond and non-planar elsewhere.

The respective C–H$_t$ distances and C–H$_t$–C bond angles at the transition states characterized here are given in Table 3. The H$_t$–C distances do not vary substantially with ring size, but the CH$_t$C angles in the transition states increase with increasing

Table 3
Transition state bond lengths and angles in H-transfers

Reaction	C1H$_t$	C2H$_t$	CH$_t$C
1 → **2**	1.224	1.641	84.4
4 → **5**	1.452	1.345	121.5
6 → **6′**	1.363	1.363	133.5

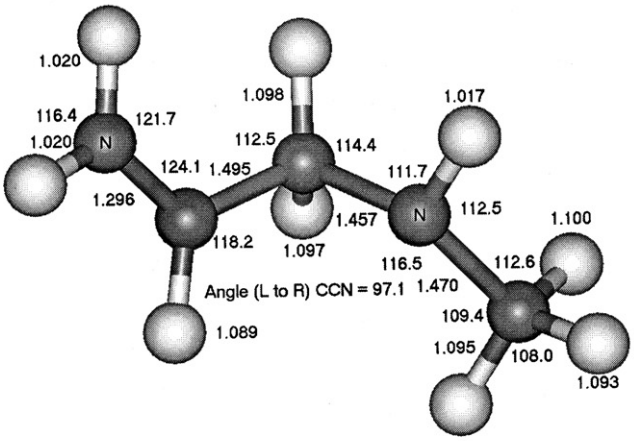

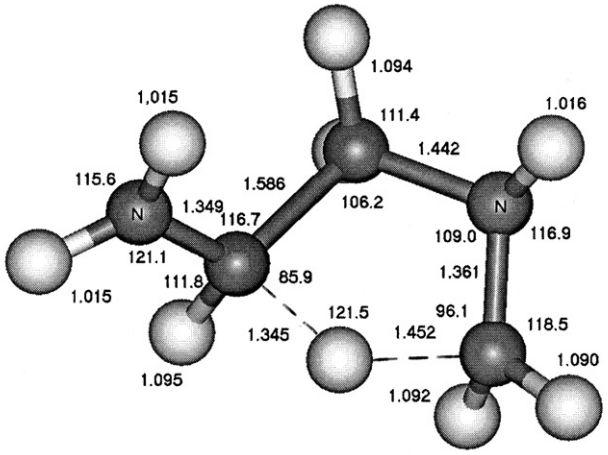

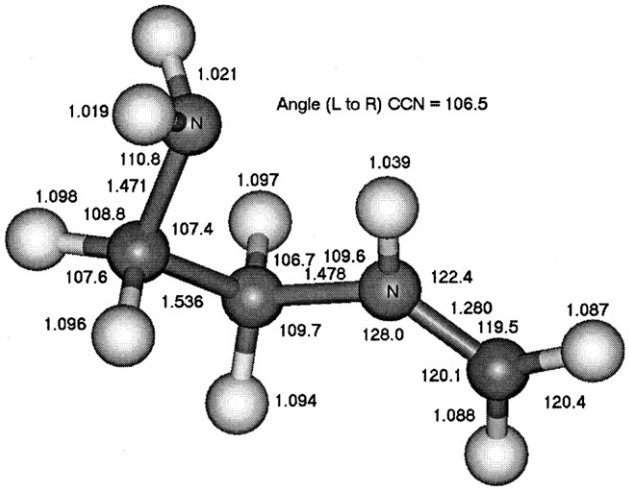

Fig. 4. Structures for $N^+H_2{=}CHCH_2NHCH_3$ (**5**) (top), $NH_2CH_2CH_2N^+H{=}CH_2$ (**4**) (bottom) and middle, the transition state connecting them (obtained by QCISD/6-31G(d) theory).

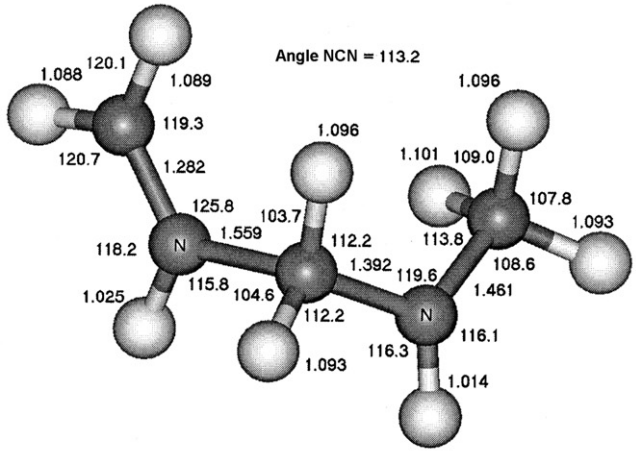

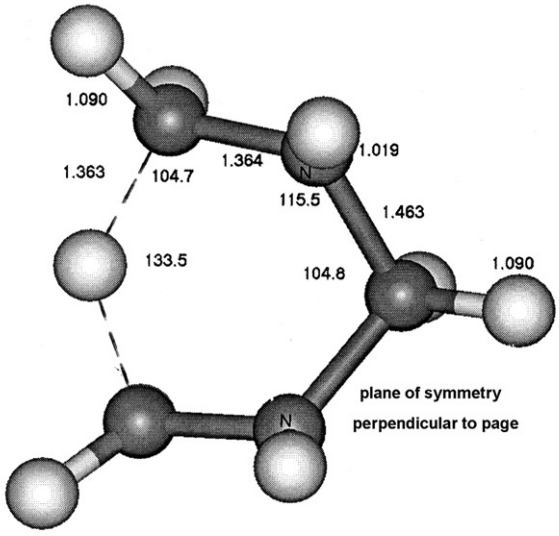

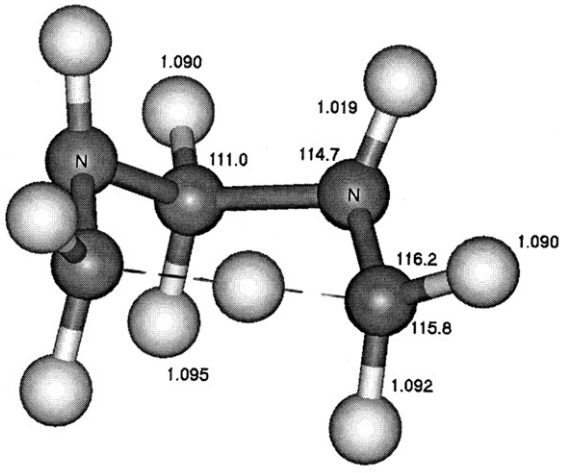

Fig. 5. Structures of $CH_3NHCH_2N^+H{=}CH_2$ (**6**) (top) and TS(**6** → **6′**) obtained by QCISD/6-31G(d) theory. The middle and bottom figures are two different views of TS(**6** → **6′**) illustrating both the symmetry of the transition state and the non-planarity of the ring for 6-membered ring H-transfer.

ring size and decreasing critical energies. Thus, the effects of conservation of orbital symmetry on the 4-membered ring H-transfers and decrease in ring strain with increasing ring size are probably the chief determinants of the critical energies and relative rates of the reactions studied here.

Acknowledgment

We thank Michael G. Hughes for help with preparation of figures.

References

[1] L.L. Griffin, K. Holden, C.E. Hudson, D.J. McAdoo, Org. Mass Spectrom. 21 (1986) 175.
[2] B.F. Yates, L. Radom, J. Am. Chem. Soc. 109 (1987) 2910.
[3] H. Budzikiewicz, C. Djerassi, D.H. Williams, Mass Spectrometry of Organic Compounds, Holden-Day, Inc., San Francisco, 1967.
[4] F.W. McLafferty, F. Tureček, Interpretation of Mass Spectrometry, fourth ed., University Science Books, Mill Valley, 1993.
[5] R.D. Bowen, Acc. Chem. Res. 24 (1991) 364.
[6] R.D. Bowen, D.H. Williams, J. Am. Chem. Soc. 100 (1978) 7454.
[7] C.E. Hudson, D.J. McAdoo, J. Am. Soc. Mass Spectrom. 18 (2007) 270.
[8] J.S. Smith, F.W. McLafferty, Org. Mass Spectrom. 5 (1971) 483.
[9] D.J. McAdoo, C.E. Hudson, Int. J. Mass Spectrom. Ion Processes 62 (1984) 269.
[10] C.E. Hudson, D.J. McAdoo, J. Am. Soc. Mass Spectrom. 15 (2004) 972.
[11] C.E. Hudson, L. Varela, L.L. Griffin, D.J. McAdoo, Int. J. Mass Spectrom. 249–250 (2006) 120.
[12] M.J. Frisch, G.W. Trucks, H.B. Schlegel, G.E. Scuseria, M.A. Robb, J.R. Cheeseman, Montgomery J.A.Jr., T. Vreven, K.N. Kudin, J.C. Burant, J.M. Millam, S.S. Iyengar, J. Tomasi, J. Barone, B. Mennucci, M. Cossi, G. Scalmani, N. Rega, G.A. Petersson, H. Nakatsuji, M. Hada, M. Ehara, K. Toyota, R. Fukuda, J. Hasegawa, M. Ishida, T. Nakajima, Y. Honda, O. Kitao, H. Nakai, M. Klene, X. Li, J.E. Knox, H.P. Hratchian, J.B. Cross, C. Adamo, J. Jaramillo, R. Gomperts, R.E. Stratmann, O. Yazyev, A.J. Austin, R. Cammi, C. Pomelli, J.W. Ochterski, P.Y. Ayala, K. Morokuma, G.A. Voth, P. Salvador, J.J. Dannenberg, V.G. Zakrzewski, S. Dapprich, A.D. Daniels, M.C. Strain, O. Farkas, D.K. Malick, A.D. Rabuck, K. Raghavachari, J.B. Foresman, J.V. Ortiz, Q. Cui, A.G. Baboul, S. Clifford, J. Cioslowski, B.B. Stefanov, G. Liu, A. Liashenko, P. Piskorz, I. Komaromi, R.L. Martin, D.J. Fox, T. Keith, M.A. Al-Laham, C.Y. Peng, A. Nanayakkara, M. Challacombe, P.M.W. Gill, B. Johnson, W. Chen, B.W. Wong, C. Gonzalez, J.A. Pople, Gaussian 03, Revision B. 04, Gaussian, Inc., Pittsburgh, PA, 2003.
[13] A.P. Scott, L. Radom, J. Phys. Chem. 100 (1996) 16502.
[14] C. Gonzalez, H.B. Schlegel, J. Chem. Phys. 90 (1989) 2154.
[15] C. Gonzalez, H.B. Schlegel, J. Phys. Chem. 94 (1990) 5523.
[16] T.L. Xhu, W.L. Hase, Quantum Chemistry Program Exchange, Chemistry Department, University of Indiana, Bloomington, 1993 (QCPE 644).
[17] C.E. Hudson, D.J. McAdoo, Am. Soc. Mass Spectrom. 9 (1998) 130.
[18] C.E. Hudson, D.J. McAdoo, Int. J. Mass Spectrom. 232 (2004) 17.
[19] C.E. Hudson, D.J. McAdoo, Int. J. Mass Spectrom. 219 (2002) 295.
[20] R.B. Woodward, R. Hoffmann, Angew. Chem. Int. 8 (1969) 781.
[21] C.E. Hudson, D.J. McAdoo, J. Org. Chem. 68 (2003) 2735.